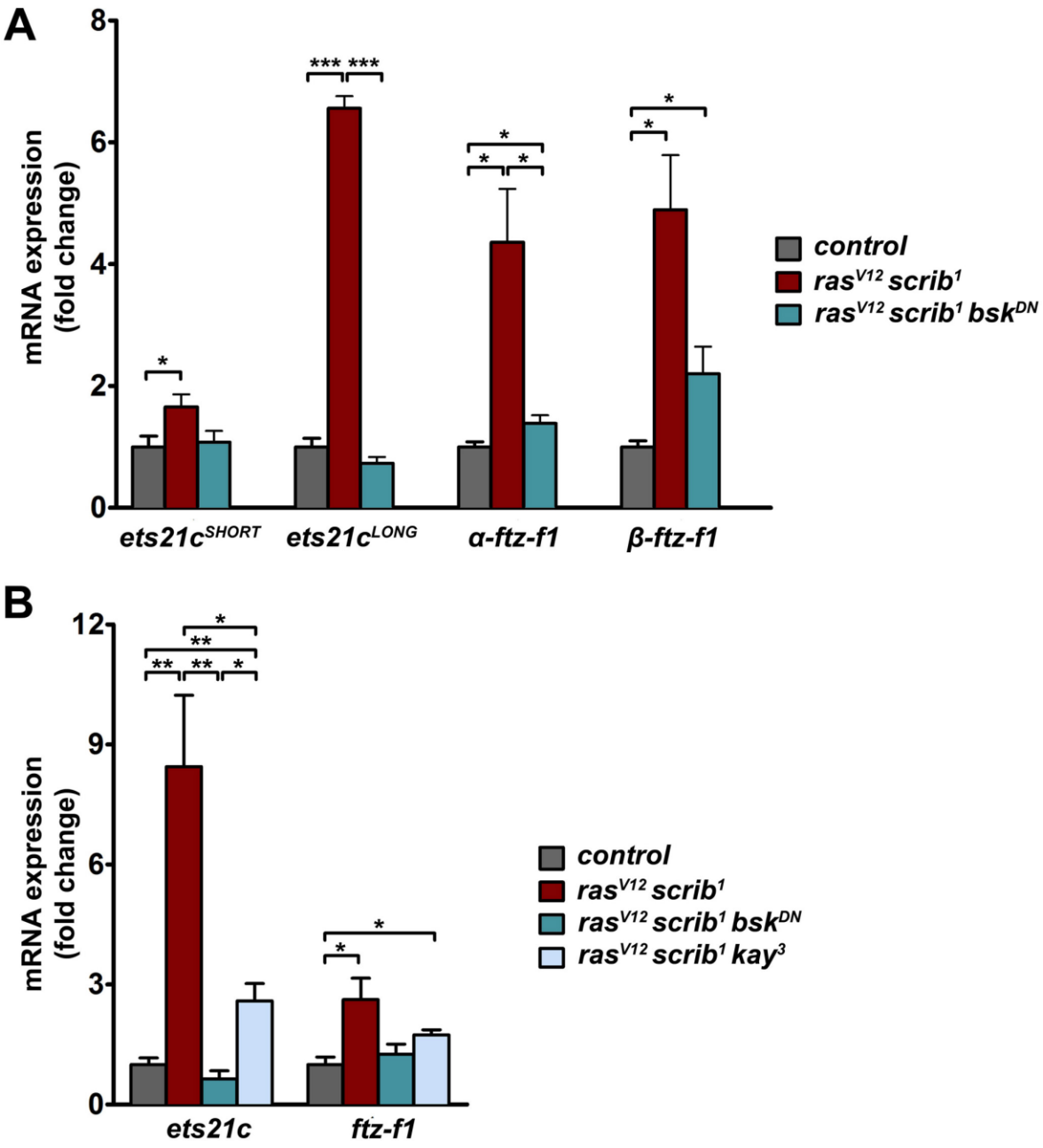

Supplementary Fig. S1. *ftz-f1* and *ets21c* transcripts are upregulated in $ras^{V12}scrib^{1}$ tumors in a JNK-Fos-dependent manner

Expression of both *ets21c* ($ets21c^{LONG}$ and $ets21c^{SHORT}$) and *ftz-f1* (*α-ftz-f1* and *β-ftz-f1*) isoforms was upregulated in EAD bearing $ras^{V12}scrib^{V12}$ tumors in a JNK-dependent manner ($ras^{V12}scrib^{1}bsk^{DN}$), albeit to a different extent as shown by qRT-PCR. **(B)** Loss of *kayak* (kay^{3}) rescued expression of *ets21c* and *ftz-f1* in $ras^{V12}scrib^{1}$ tumors, mimicking the effect of JNK inhibition ($ras^{V12}scrib^{1}bsk^{DN}$). Data are mean ± s.e.m.; n = 3-5; ***p<0.001; **p<0.005; *p<0.01.

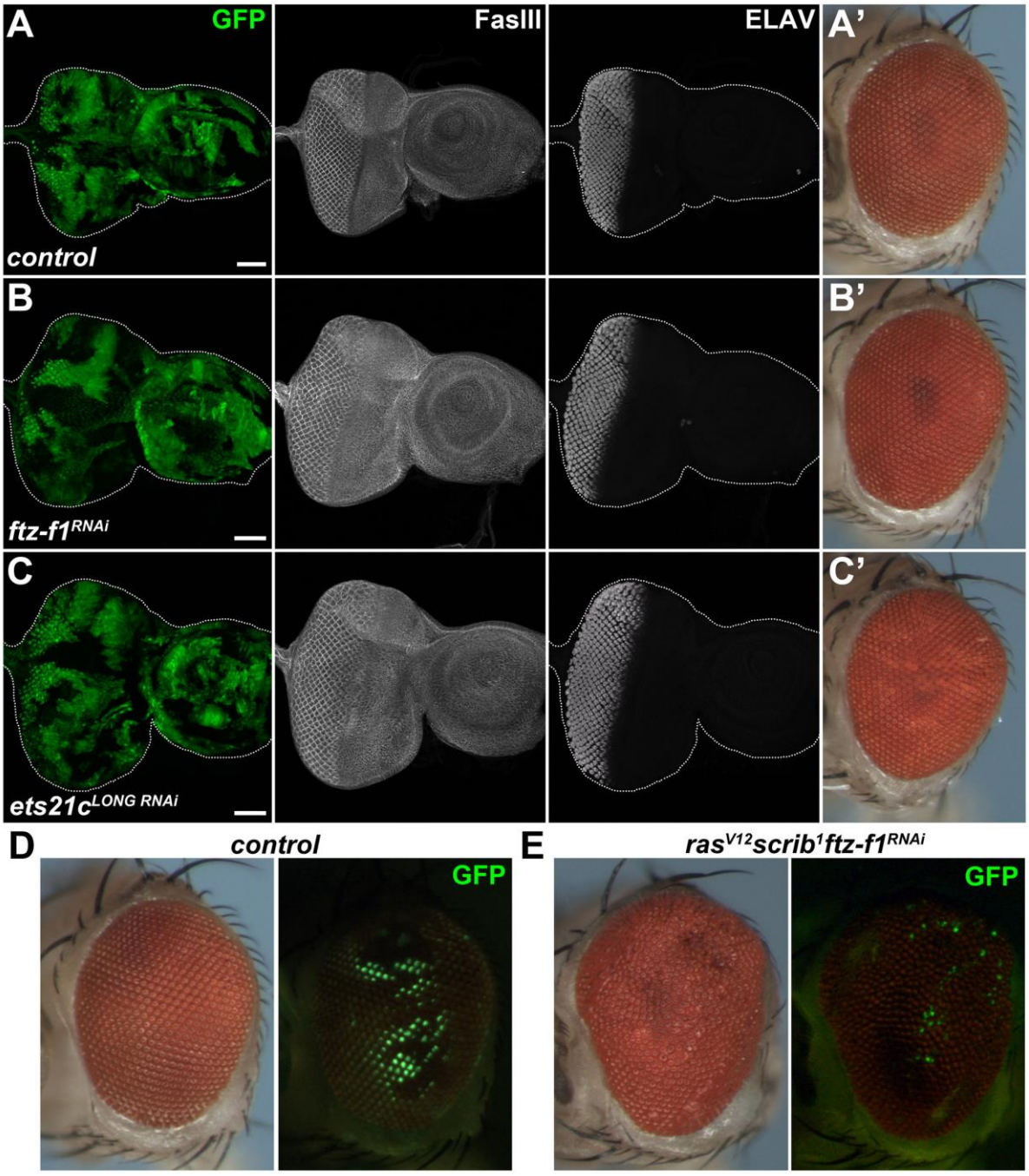

Supplementary Fig. S2. RNAi mediated knockdown of *ftz-f1* and *ets21c* does not affect normal eye development

(A-C) Knockdown of *ftz-f1* (B) or *ets21c*^{LONG} (C) in clones of the EAD had no obvious impact on EAD morphology (marked by FasIII), photoreceptor differentiation (marked by ELAV) or adult eye development (A'-C'). Images show EAD as projections of multiple confocal sections 6 days AEL. **(D-E)** Adult eyes of animals bearing *ras*^{V12}*scrib*^{1}*ftz-f1*^{RNAi} are larger than control. Yet most of the ommatidia are GFP negative, indicating expansion of non-clonal tissue. Scale bars: 50 μm (A-C).

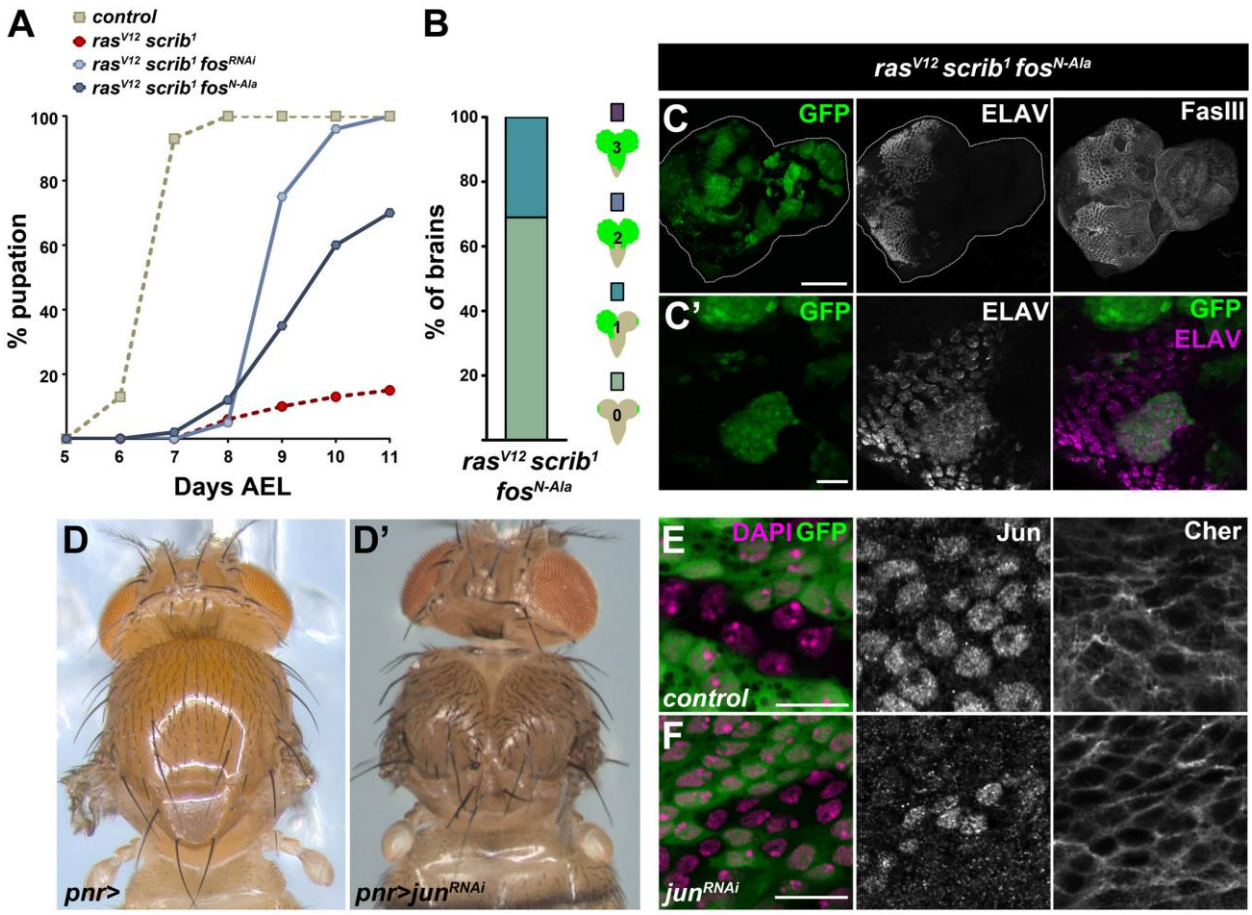

Supplementary Fig. S3. JNK-mediated phosphorylation of Fos is critical to its oncogenic activity in *ras^{V12}scrib^{1}* tumors

(A) Similar to *fos* inhibition via RNAi**,** expression of *fos$^{N\text{-}Ala}$* mutant bearing substitutions of the N-terminal JNK specific phosphorylation sites with alanine in *ras^{V12}scrib^{1}* clones markedly improved pupation rate (p<0.0001) compared to animals bearing *ras^{V12}scrib^{1}* tumors. The graph shows cumulative percentage of pupae forming over time. Dashed lines are repeated from Fig. 3. **(B)** Introduction of *fos$^{N\text{-}Ala}$* into *ras^{V12}scrib^{1}* clones suppressed their invasiveness (see Fig. 3 for comparison with *ras^{V12}scrib^{1}*). Four grades of invasiveness were scored based on spreading of clonal GFP-positive cells into larval brains dissected on day 7 AEL. Results are percentage of brains falling into each category. **(C)** While overexpression of *fos$^{N\text{-}Ala}$* in *ras^{V12}scrib^{1}* did not reduce the size of GFP-labeled clones, it partly rescued ELAV expression. (**D**) *Pannier-GAL4* (*pnr>)* driven *jun^{RNAi}* recapitulates a previously reported thorax cleft phenotype (Jindra et al., 2004). (**E-F**) RNAi knockdown of *jun* in GFP-positive EAD clones results in a depletion of its protein product relative to the surrounding wild-type tissue. Images show EAD dissected 6 days AEL, either as projections of multiple confocal sections (C) or close-up single sections (C', E, F). Scale bars: 100 μm (C), 20 μm (C') and 10 μm for (E, F).

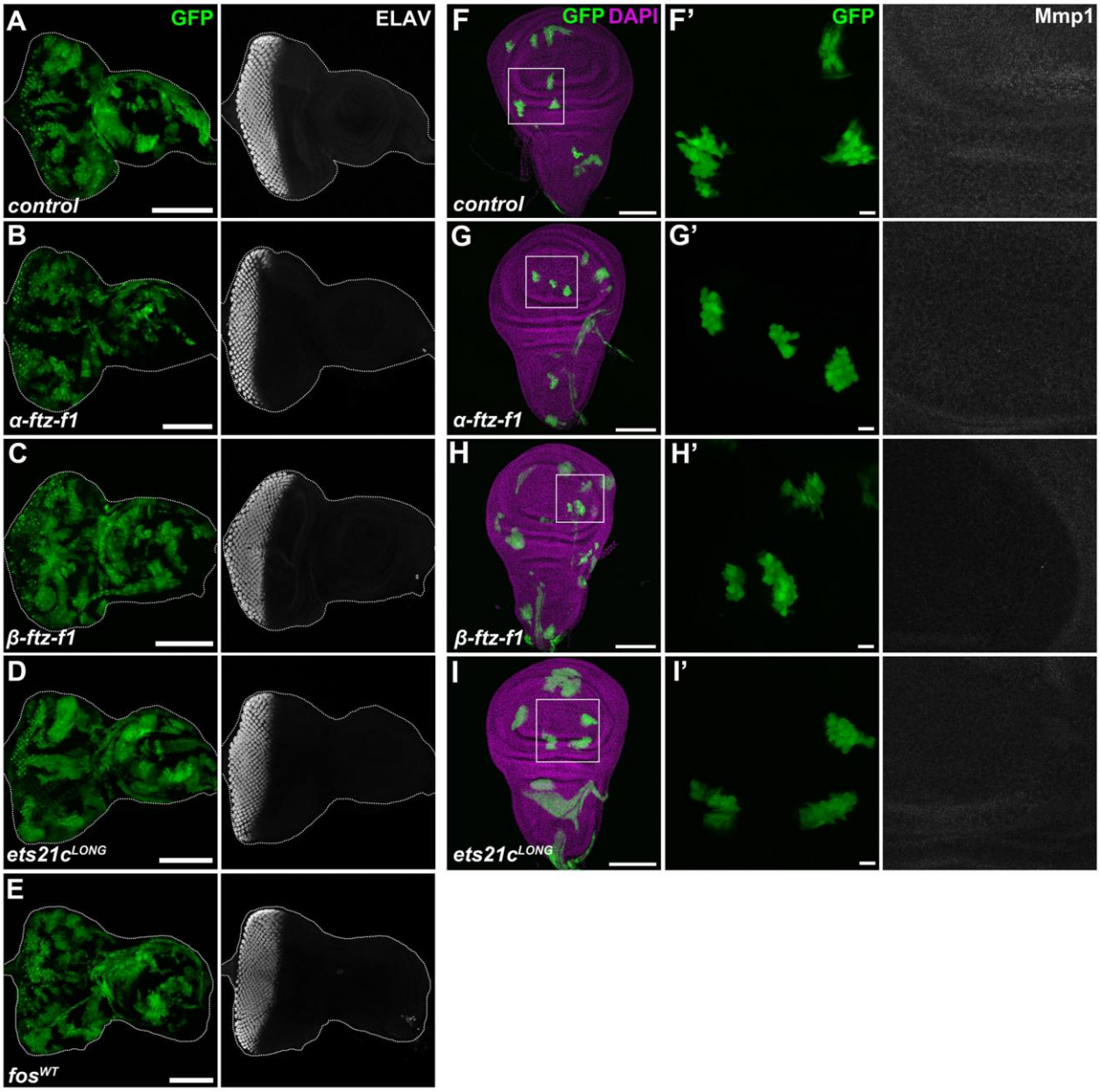

Supplementary Fig. S4. Clonal overexpression of individual TFs is insufficient to induce MMP1 and causes no obvious phenotypes.

(A-E) Similar to GFP-labeled control EAD clones (A), overexpression of *α-ftz-f1* (B), *β-ftz-f1* (C), *ets21c*^{LONG} (D) or *fos*^{WT} (E) affected neither clone size nor their morphology or photoreceptor differentiation marked by ELAV. **(F-I)** Similar to control (F), overexpression of *α-ftz-f1* (G), *β-ftz-f1* (H) or *ets21c*^{LONG} (I) in clones of wing imaginal discs altered neither clonal morphology nor MMP1 expression (F'-I'). Images are projections of multiple confocal sections of EAD and wing discs on day 6 AEL. Scale bars: 100 μm (A-I) and 10 μm (F'-I').

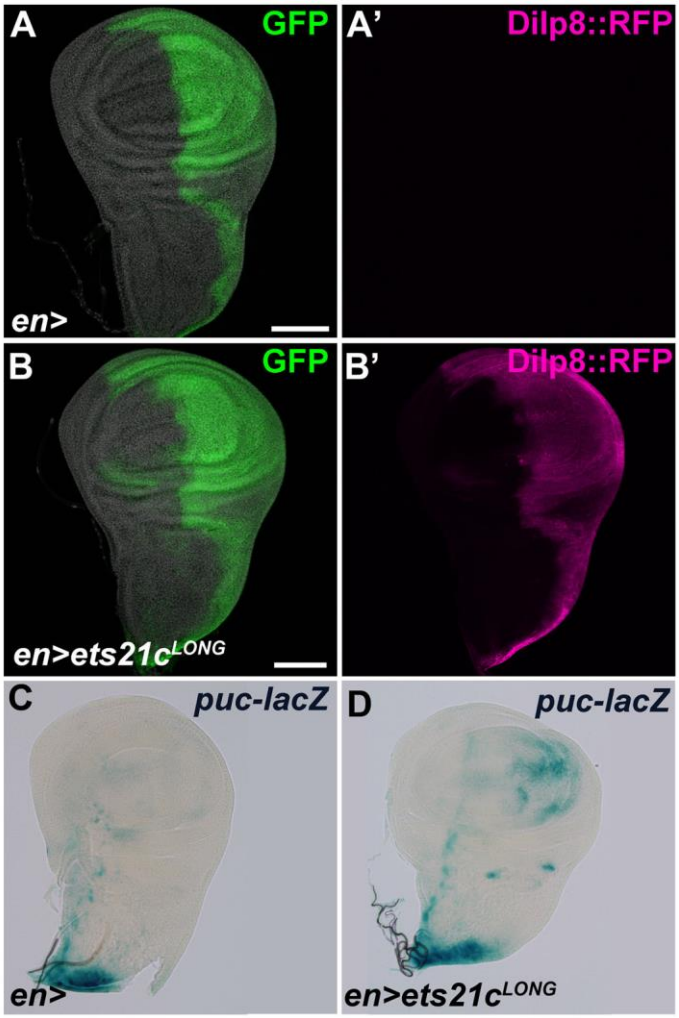

Supplementary Fig. S5. Ets21c is sufficient to induce *dilp8* and *puc* expression

(A-D) Overexpression of *ets21c* in the posterior compartment of the wing imaginal disc using *engrailed-GAL4, UAS-GFP* driver (*en>GFP*) is sufficient to upregulate Dilp8::RFP expression (B') and activity of *puc::lacZ* reporter (D). Nuclei are visualized with DAPI. All images show wing disc 6 days AEL as projections of multiple confocal sections. Scale bars: 100 µm.

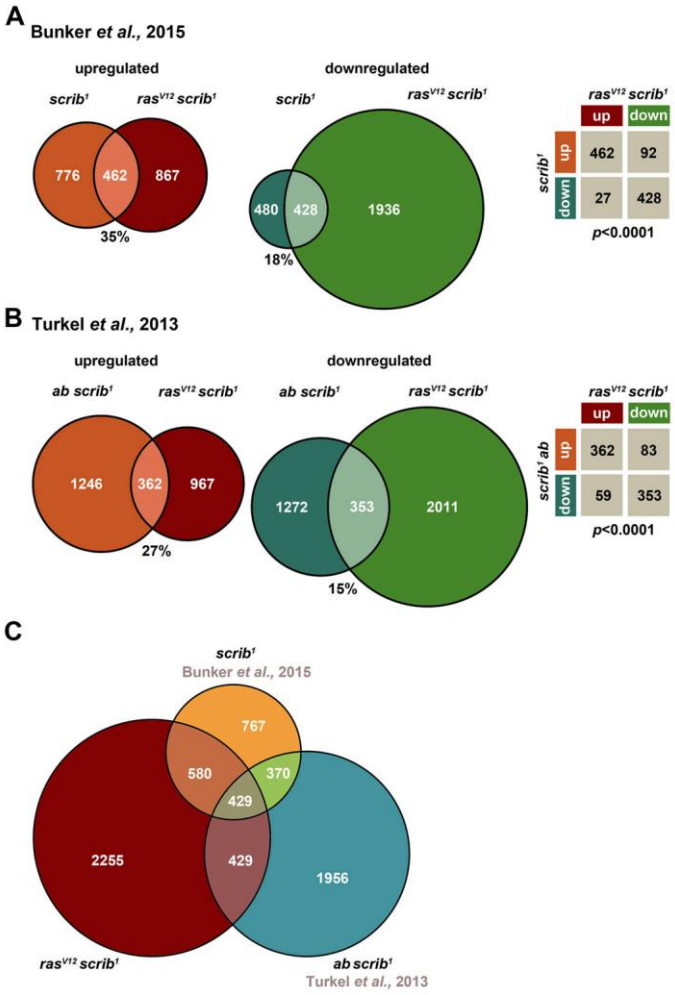

Supplementary Fig. S6. Tumors with compromised epithelial polarity share "Polarity response transcriptional signature"

(**A-C**) Venn diagrams depict overlap of deregulated genes between mosaic EAD bearing malignant *ras*^{V12}*scrib*^{1} clones (our study), overgrown *scrib*^{1} mutant wing discs (Bunker et al., 2015) or *abrupt scrib*^{1} EAD clonal tumors (Turkel et al., 2013). To determine the intersections between different gene expression datasets, we used cut-off of +/-1.5-fold change compared to control for all datasets. The percentages of overlap are given from the perspective of genes regulated in *ras*^{V12}*scrib*^{1} that match the other datasets. Contingency tables provide information about directionality of the expression of common transcripts and serve to calculate the significance of overlap using a two-tailed Fisher Exact Probability test. For list of genes see Table S1.

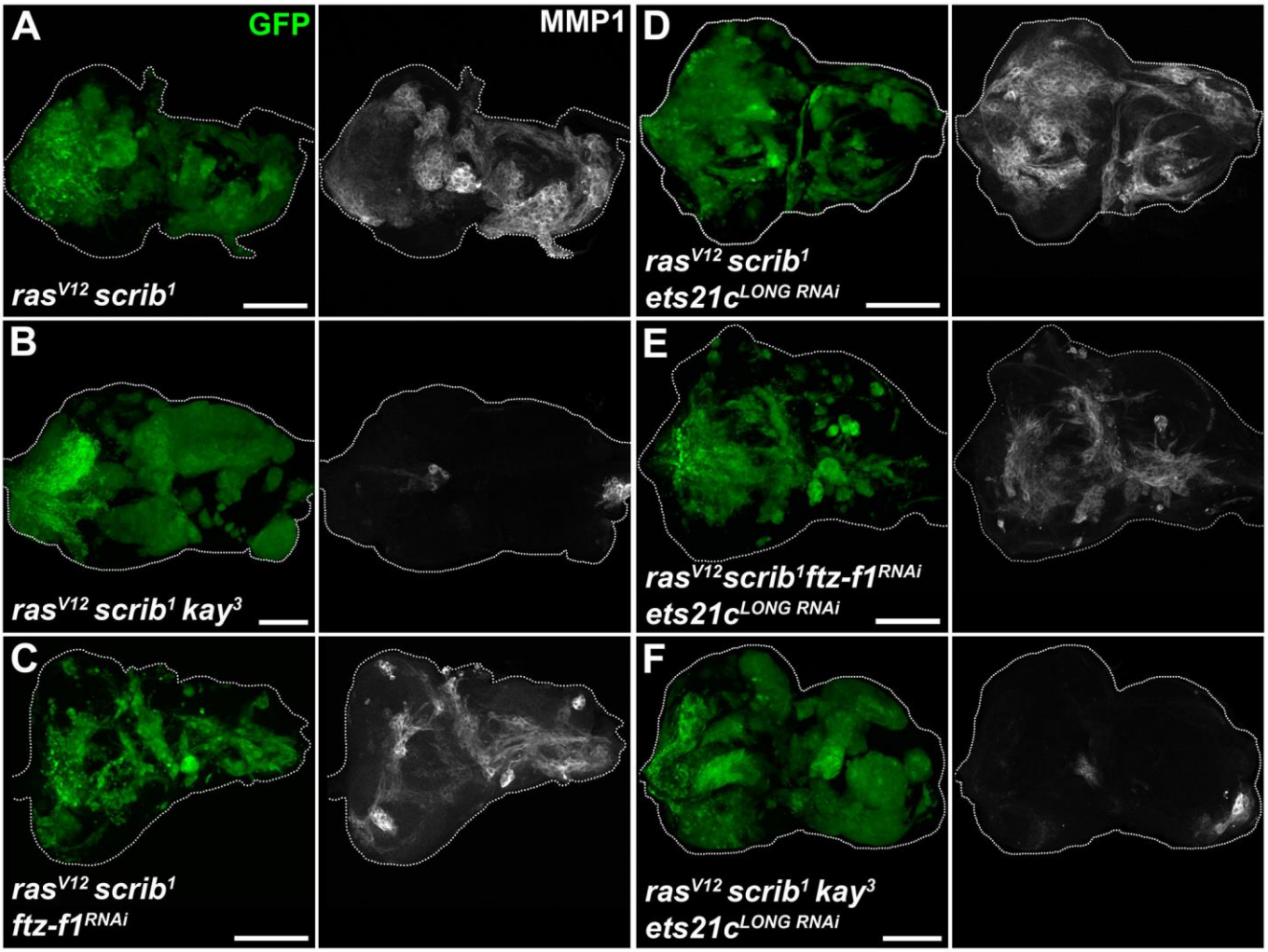

Supplementary Fig. S7. Fos is the master regulator of MMP1 expression

(A-F) Loss of Fos resulted in dramatic downregulation of MMP1 in clonal tissue while knockdown of *ets21c* or *ftz-f1* or both had no effect. All images show EAD 6 days AEL as projections of multiple confocal sections. Scale bars: 100 μm (A-F).

Supplementary tables

Supplementary Table S1. List of differentially expressed genes, enriched GO term clusters, and TF motif analysis and comparative analysis of tumor transcriptomes

Click here to Download Table S1

Supplementary Table S2. Primer sets for quantitative reverse transcription-PCR (qRT-PCR) and cloning of *ets21c*^{LONG}

	Forward primers (5'=>3')	Reverse primers (5'=>3')
	qRT-PCR	
rp49	TCCTACCAGCTTCAAGATGAC	CACGTTGTGCACCAGGAACT
ets21c^{SHORT}	ATGAGCGTCAGCGTGGACG	GAAGATCATCGAGGTGTGCGGATG
ets21c^{LONG}	ATTAATGCCATGCATCAGGATGTCCG	GTGGGAACTTCCGTCTCCTTCG
ets21c	ACATGAACTACGACAAGCTGAGCC	CGTGCACCTTGGTCATGATGTTCT
α-ftz-f1	GGATACCTTCAATGTACCTATGC	GATGATGGGGCATTAGGAGTTG
β-ftz-f1	GACCGTACAGTTTATATCGTCGC	CGTGTAGGCATTGTATTCGTGC
ftz-f1	TCCCTACTGCCGATTCCAGAAG	TGTACATGGGTCCGAATTTGTTGC
dilp8	GCACAACAAGCATCACTACATCA	GTTGTAGGACCTGCTCGAGTG
mmp1	AGGGCGACAAGTACTACAAGCTGA	ACGTCTTGCCGTTCTTGTAGGTGA
puc	CTTCGTCACATGCCAGATTCTC	AGGCTACTACAGTTAAAAAAGGC
cher	ACAAACCCGTGATCCAGGACAA	AGGCCGGGTCCGTAGGCAG
upd3	AGTGAGCACCAAGACTCTGGACAT	GTGGCGAAGGTTCAACTGTTTGCT
	pTMW UAS-based construct	
ets21c^{LONG}	AAGAATTCTAATGGCCATTCTACAGAATAGCCGC	AACTCGAGTCAGTTGAATGCATTTGTGGTGG

Supplementary Table S3. List of genotypes used for clonal analyses

MOSAIC ANALYSES	
hsFLP; act>y^{+}>GAL4, UAS-GFP/CyO	*ey-FLP1; act>y^{+}>GAL4, UAS-GFP; FRT82B, Tub-GAL80*
w^{1118}	*w;; FRT82B*
w; UAS-α-ftz-f1	*w; UAS-ras^{V12}; FRT82B/TM6B*
w; UAS-β-ftz-f1	*w; UAS-ras^{V12}; FRT82B scrib^{1}/TM6B*
w; UAS-Myc-ets21c^{LONG}	*w; UAS-ras^{V12}; FRT82B scrib^{1} UAS-bsk^{DN}/TM6B*
	w; UAS-ras^{V12}; FRT82B scrib^{1} UAS-fos$^{35/19\ RNAi}$/TM6B
	w; UAS-ras^{V12}; FRT82B scrib^{1} kay^{3}/TM6B
	w; UAS-ras^{V12} UAS-jun^{RNAi}; FRT82B scrib^{1} /TM6B
	w; UAS-ras^{V12}; FRT82B scrib^{1} UAS-ftz-f1^{RNAi}/TM6B
	w; UAS-ras^{V12} UAS-ets21c$^{LONG\ RNAi}$; FRT82B scrib^{1}/TM6B
	w; UAS-ras^{V12} UAS-α-ftz-f1; FRT82B/TM6B
	w; UAS-ras^{V12} UAS-β-ftz-f1; FRT82B/TM6B
	w; UAS-Myc-ets21c^{LONG}; FRT82B/TM6B
	w;; UAS-ftz-f1^{RNAi} FRT82B/TM6B
	w; UAS-ets21c$^{LONG\ RNAi}$; FRT82B/TM6B
	w; UAS-ras^{V12} UAS-ets21c$^{LONG\ RNAi}$; FRT82B scrib^{1} kay^{3}/TM6B
	w; UAS-ras^{V12} UAS-ets21c$^{LONG\ RNAi}$; FRT82B scrib^{1} UAS-ftz-f1^{RNAi}/TM6B
	w; UAS-ras^{V12} UAS-fos^{WT}; FRT82B/TM6B
	w; UAS-α-ftz-f1; FRT82B/TM6B
	w; UAS-β-ftz-f1; FRT82B/TM6B
	w; UAS-ras^{V12} UAS-Myc-ets21c^{LONG}; FRT82B/TM6B
	w; UAS-ras^{V12} UAS-Myc-ets21c^{LONG}; FRT82B UAS-bsk^{DN}/TM6B
	w; UAS-ras^{V12} ex::lacZ; FRT82B scrib^{1}/ TM6B
	w; UAS-ras^{V12} ex::lacZ; FRT82B scrib^{1} UAS-ftz-f1^{RNAi}/ TM6B
	w; UAS-ras^{V12} ex::lacZ; FRT82B scrib^{1} kay^{3}/TM6B